Transition-Metal Hydrides

DOI: 10.1002/anie.201205209

Open-Shell First-Row Transition-Metal Polyhydride Complexes Based on the *fac*-$[RuH_3(PR_3)_3]^-$ Building Block**

*Markus Plois, Waldemar Hujo, Stefan Grimme, Christian Schwickert, Eckhard Bill, Bas de Bruin, Rainer Pöttgen, and Robert Wolf**

Although hydride, H^-, is the simplest conceivable ligand,[1] transition-metal hydride complexes continue to fascinate synthetic and theoretical chemists owing to their intriguing structures, unusual reactivities, and diverse bonding patterns.[2,3] Metal hydrides are implicated in a plethora of catalytic processes, such as hydrogenation, hydroformylation, and isomerization reactions.

The vast majority of molecular hydrides are diamagnetic closed-shell species. Polyhydride transition-metal complexes with an open-shell electron configuration are comparatively rare.[4] Their relative instability compared to closed-shell derivatives has been attributed to various decomposition pathways.[5] Paramagnetic hydride species are nevertheless interesting catalytic intermediates of hydrogenase and nitrogenase enzymes.[6] Oligonuclear polyhydride complexes are of interest because of their potential ability to activate organic and inorganic molecules in a cooperative fashion by using two or more metal centers.[7] However, only a small number of paramagnetic polyhydrido transition-metal clusters has been characterized to date.[8]

We wondered whether the *fac*-$[RuH_3(PR_3)_3]^-$ anion **A** (Figure 1) might be a suitable building block for unprecedented paramagnetic hydride complexes with a heterobimetallic architecture. The phenyl derivative *fac*-$[RuH_3(PPh_3)_3]^-$ was previously characterized as the potassium salt $[K([18]crown-6)][Ru(\mu\text{-}H)_3(PPh_3)_3]$.[9] The molecular structure of anion *fac*-$[RuH_3(PPh_3)_3]^-$ displays a facial trihydrido ruthenium unit that should be able to bind a second transition-metal cation. Interestingly, the anion could not be incorporated successfully into stable bimetallic polyhydrido complexes when treated with $[\{RhCl(cod)\}_2]$ (cod = 1,5-cyclooctadiene) and $[\{IrCl(cod)\}_2]$.[10] Instead, rearrangement products **B** and **C** (Figure 1) were isolated.

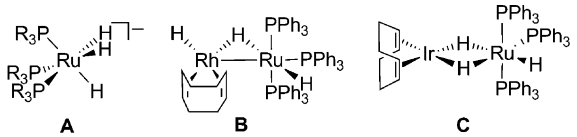

Figure 1. Facial trihydrido ruthenium moiety **A** and rearrangement products **B** and **C**.

Herein, we report the synthesis and full characterisation of the new, paramagnetic polyhydride complexes $[Fe(acac)\{Ru(\mu\text{-}H)_3(PTol_3)_3\}]$ (**FeRu**), and $[M\{Ru(\mu\text{-}H)_3(PTol_3)_3\}_2]$ (**MRu_2**, M = Cr-Ni) (Scheme 1). The diamagnetic zinc complex $[Zn\{Ru(\mu\text{-}H)_3(PTol_3)_3\}_2]$ (**$ZnRu_2$**) is also described for comparison. The reported complexes are remarkable because 1) they are rare examples of heterometallic transition-metal polyhydride complexes which contain a first-row transition-metal ion; 2) they show intriguing structural and spectroscopic features; and 3) the complexes are rare open-shell hydride complexes where the metal ion has a high-spin configuration.

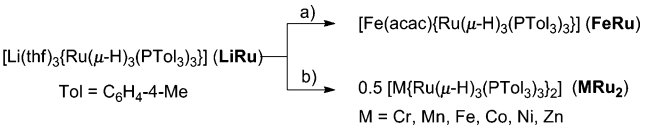

Scheme 1. Synthesis of new polyhydride complexes **FeRu** and **MRu_2**. Reagents: a) $[Fe(acac)_2]$; b) $Cr(OAc)_2$, $[MnCp_2]$, $[Fe(acac)_2]$, CoI_2, $[Ni(acac)_2]$, and $ZnCl_2$ (0.5 equivalent with respect to **LiRu**).

[*] M. Plois, C. Schwickert, Prof. Dr. R. Pöttgen, Prof. Dr. R. Wolf
Universität Münster
Institut für Anorganische und Analytische Chemie
Corrensstrasse 30, 48149 Münster (Germany)
M. Plois, Prof. Dr. R. Wolf
Universität Regensburg, Institut für Anorganische Chemie
93040 Regensburg (Germany)
E-mail: robert.wolf@ur.de
W. Hujo
Universität Münster, Institut für Organische Chemie
Corrensstrasse 40, Münster 48149 (Germany)
Prof. Dr. S. Grimme
Universität Bonn, Mulliken Center für Theoretische Chemie
Institut für Physikalische und Theoretische Chemie
Beringstrasse 4, 53115 Bonn (Germany)
Dr. E. Bill
Max Planck Institute for Chemical Energy Conversion
Stiftstrasse 34–36, 45470 Mülheim an der Ruhr (Germany)
Dr. B. de Bruin
University of Amsterdam (UvA)
Van 't Hoff Institute for Molecular Sciences (HIMS)
Science Park 904, 1098 XH Amsterdam (The Netherlands)

[**] We thank S. Pelties, M. Eilers-Rethwisch, K. Schäfer, J. Malberg, and H. Kruse for assistance and helpful discussions. S. Demeshko and F. Meyer (University of Göttingen) are thanked for collecting and analyzing magnetic data. Support by the Deutsche Forschungsgemeinschaft within the framework of the SFB 858 ("Synergetische Effekte in der Chemie—Von der Additivität zur Kooperativität.") is gratefully acknowledged. Johnson Matthey is thanked for a generous loan of ruthenium trichloride. R.W. thanks Prof. Dr. W. Uhl for his support.

Supporting information for this article is available on the WWW under http://dx.doi.org/10.1002/anie.201205209.

The lithium salt $[Li(thf)_{2.5}\{Ru(\mu\text{-}H)_3(PTol_3)_3\}]$ (**LiRu**), which carries *para*-tolyl substituents (Tol) for better solubility, was used as the precursor to the oligonuclear complexes targeted in this study. **LiRu** can be prepared in 65% yield by reacting $[RuCl_2(PTol_3)_3]$ with three equiv of $LiBEt_3H$. The facial stereochemistry of the *fac*-$[RuH_3(PTol_3)_3]^-$ anion of **LiRu** was confirmed by ^1H and ^{31}P NMR spectroscopy and a single-crystal X-ray diffraction study (Supporting Information, Figure S1).[11,12]

The dinuclear complex $[Fe(acac)\{Ru(\mu\text{-}H)_3(PTol_3)_3\}]$ (**FeRu**) was obtained by reacting **LiRu** with one equiv $[Fe(acac)_2]$ (43% yield, Scheme 1a).[12] The molecular structure of air-sensitive, orange **FeRu** (Figure 2) was determined by X-ray crystallography.[11,12] The hydride ligands were located in the Fourier difference map and refined freely. The crystallographic refinement is further supported by the close agreement with the DFT-optimized (PBE-D3/def2-TZVP level)[12–14] structure of $[Fe(acac)\{Ru(\mu\text{-}H)_3(PTol_3)_3\}]$ (**FeRu**). The structure of **FeRu** shows an intact *fac*-$[RuH_3(PTol_3)_3]^-$ anion that coordinates to iron in a symmetric fashion by three bridging hydrides. The ruthenium atom shows a distorted octahedral geometry similar to that in the lithium salt **LiRu**. The coordination sphere of iron is completed by one acetylacetonato (acac) ligand, resulting in coordination number five for iron.

Reactions of two equiv of **LiRu** with various divalent transition-metal salts yielded the trinuclear complexes $[M\{Ru(\mu\text{-}H)_3(PTol_3)_3\}_2]$ (**MRu_2**, M = Cr, Mn, Fe, Co, Ni, and Zn) in moderate yields (18–41%, Scheme 1b).[12] The compounds could be isolated as air-sensitive, crystalline solids and were fully characterized. Single-crystal X-ray crystallography showed that the complexes are isostructural and feature a unique $\{Ru(\mu\text{-}H)_3M(\mu\text{-}H)_3Ru\}$ structural motif with a linear arrangement of the three metal atoms.[11,12] The structure of the iron complex **$FeRu_2$** is depicted as an example in Figure 2. The structural parameters (Table 1) obtained by X-ray crystallography are in close agreement with the DFT-optimized structures of the model complexes $[M\{Ru(\mu\text{-}H)_3(PPh_3)_3\}_2]$ (**MRu_2'**), where the Me groups of the *para*-tolyl ligands were omitted for computational efficiency.[12–15] Interestingly, the central, hexacoordinate 3d metal shows a trigonally distorted octahedral coordination environment with H-M-H angles, which deviate strongly from the 90° angles expected for a regular octahedron (Table 1). The M–H bonds are consistently about 0.2 Å longer than the Ru–H bonds. The latter are in the range of values observed for other ruthenium(II) hydride complexes.[16] The calculated M–H and Ru–H distances deviate by less than 0.01 Å from the mean value except for the chromium complex **$CrRu_2'$**, which shows somewhat larger differences between the individual M–H and Ru–H bonds (Cr–H 1.88 and 2.00 Å, Ru–H 1.67, 1.71, and 1.72 Å).

Only few homoleptic first-row transition-metal polyhydride complexes have been described.[17] The octahedral $[FeH_6]^{4-}$ anion has been observed in the solid-state structures of $[MgX(thf)_2]_4[FeH_6]$ (X = Cl, Br; Fe–H distance determined by neutron diffraction: 1.609(2) Å) and M_2FeH_6 (M = Mg, Ca, Sr; Fe–H range 1.53–1.74 Å).[18] The Fe–H bonds in these compounds are approximately 0.2 Å shorter than the Fe–H distances determined in the X-ray structures of **FeRu** and **$FeRu_2$** (Figure 2 and Table 1). The structure of the recently reported pentanuclear manganese cluster $[\{Cp'Mn\}_4\{MnH_6\}]$ ($Cp' = 1,2,4\text{-}(Me_3C)_3C_5H_2$) features an octahedral $[MnH_6]^{4-}$ anion with an average Mn–H distance of 1.57(3) Å.[19] The trinuclear nickel complex $K_2[LNi(\mu\text{-}H)_2Ni(\mu\text{-}H)_2NiL]$ (L = bulky diketiminato ligand) shows a planar Ni_3H_4 core with relatively short Ni–H distances of 1.47(3) and 1.62(3) Å (cf. the average Ni–H distance of 1.75(3) Å in **$NiRu_2$**).[20] Furthermore, the stabilization of a $[SiH_6]^{2-}$ anion has been observed in the complex $[\{PhBP^{Ph}_3\}Ru]_2(\mu\text{-}\eta^3\text{:}\eta^3\text{-}$

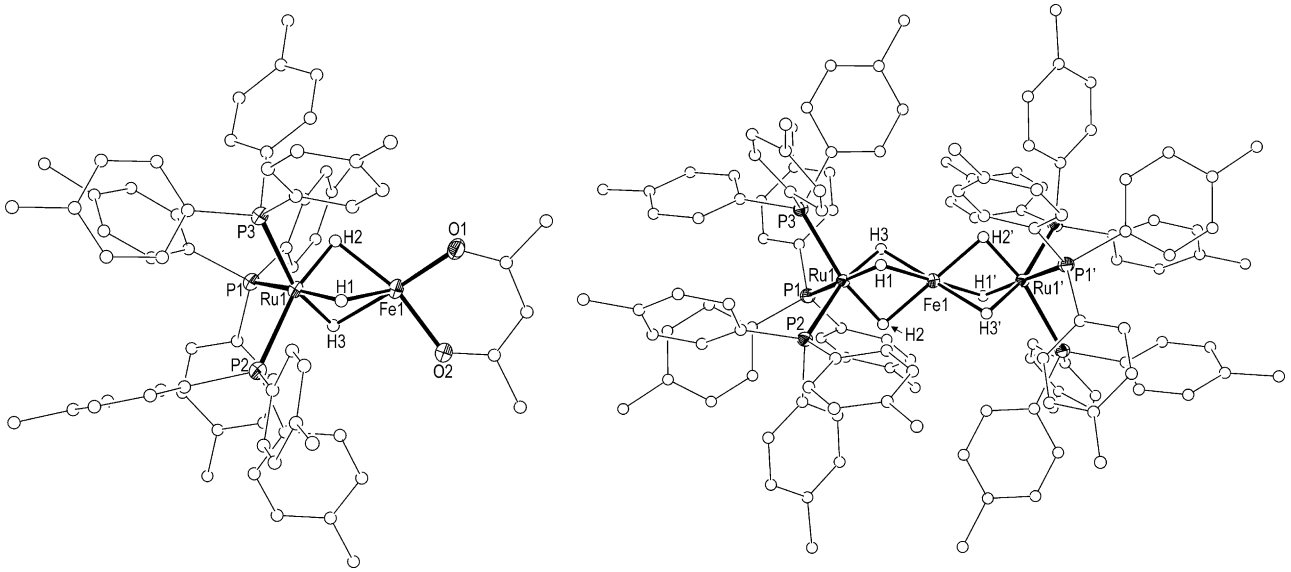

Figure 2. Solid-state molecular structure of complex $[Fe(acac)\{Ru(\mu\text{-}H)_3(PTol_3)_3\}]$ (**FeRu**, left) and $[Fe\{Ru(\mu\text{-}H)_3(PTol_3)_3\}_2]$ (**$FeRu_2$**, right). Hydrogen atoms except H1–H3 have been omitted for clarity. Ellipsoids are set at 50% probability. Selected bond lengths [Å] for **FeRu**: Ru1–P1 2.3381(5), Ru1–P2 2.3738(4), Ru1–P3 2.3720(4), Fe1–O1 2.0068(12), Fe1–O2 2.0031(12), Ru1–H1 1.66(2), Ru1–H2 1.64(2), Ru1–H3 1.66(2), Fe1–H1 1.96(2), Fe1–H2 1.99(2), Fe1–H3 1.97(2). Selected bond lengths for **$FeRu_2$** are given in Table 1.

Table 1: Selected bond lengths [Å] and angles [°] for complexes [M{Ru(μ-H)$_3$(PTol$_3$)$_3$}$_2$] (**MRu$_2$**, M = Cr–Ni, Zn) as determined by X-ray crystallography. Structural parameters for the optimized geometries (PBE-D3/def2-TZVP level) of [M{Ru(μ-H)$_3$(PPh$_3$)$_3$}$_2$] (**MRu$_2$′**) are given in square brackets.

	Cr	Mn	Fe	Co	Ni	Zn
Ru–H[a]	1.65(3) [1.70]	1.70(3) [1.68]	1.67(2) [1.69]	1.68(3) [1.70]	1.68(3) [1.71]	1.80(4) [1.67]
Ru–P[a]	2.3383(5) [2.33]	2.3372(6) [2.34]	2.3466(5) [2.34]	2.3377(9) [2.34]	2.3359(6) [2.32]	2.3382(10) [2.34]
M–H[a]	1.99(3) [1.92]	2.03(3) [1.95]	1.93(2) [1.88]	1.83(3) [1.82]	1.75(3) [1.82]	2.09(4) [1.95]
Ru–M	2.55069(16) [2.53]	2.5389(6)[a] [2.52]	2.50129(17) [2.46]	2.4523(3) [2.43]	2.42172(18) [2.45]	2.42472(10)[a] [2.43]
H-M-H	68.0[b] [71.1], 111.7[c] [108.9]	70.5[d] [70.5], 109.4[e] [109.5]	70.6[b] [72.8] 109.4[c] [107.1]	72.3[b] [74.7], 107.5[c] [105.2]	73.9[b] [74.3], 106.1[c] [105.7]	77.0[d] [72.7], 102.1[e] [107.3]

[a] Average over all bonds. [b] Average H1-M1-H2, H1-M1-H3, H2-M1-H3. [c] Average H1-M1-H2′, H1-M1-H3′, H2-M1-H3′. [d] Average H1-M1-H2′, H1-M1-H2″, H3-M2-H3′. [e] Average H1-M1-H2, H1-M1-H2″, H3-M2-H3‴.

SiH$_6$)], which contains two triphosphanylborate ruthenium fragments.[21]

The most noticeable structural differences between the trinuclear complexes **MRu$_2$** are observed for the Ru-M distances, which monotonically decrease from 2.55069(16) Å (M = Cr) to 2.42472(10) Å (M = Zn). Although these Ru-M separations are in the range that could be expected for a ruthenium-3d metal bond, a direct electronic interaction between ruthenium and the central 3d metal ion is not revealed in our DFT calculations (see below).

Complexes **MRu$_2$** (M = Cr–Ni) show high effective magnetic moments per formula unit (determined by Evans' method in [D$_8$]THF solution) of 4.6(1) μ_B (**CrRu$_2$**), 5.9(1) μ_B (**MnRu$_2$**), 5.6(1) μ_B (**FeRu$_2$**), 4.5(1) μ_B (**CoRu$_2$**), and 3.2(1) μ_B (**NiRu$_2$**). Magnetic susceptibility data recorded on polycrystalline samples of **MnRu$_2$**, **FeRu$_2$**, **CoRu$_2$**, and **NiRu$_2$** in the temperature range 3–305 K with an external magnetic field of 10 kOe additionally confirm that the complexes have a high-spin configuration in the solid state.[12] Except for the chromium and the manganese complex, the effective magnetic moments observed at 295 K are larger than the spin-only values $\mu_{s.o.}$ for divalent 3d metal ions in high-spin states, which are $\mu_{s.o.}$ = 4.90 μ_B (Cr^{II}, S = 2), 5.92 μ_B (Mn^{II}, S = 5/2), 4.90 μ_B (Fe^{II}, S = 2), 3.87 μ_B (Co^{II}, S = 3/2) and 2.82 μ_B (Ni^{II}, S = 1). Similarly, the effective magnetic moment of dinuclear **FeRu** (5.2(1) μ_B, [D$_8$]THF solution) is larger than the expected spin-only value for a high-spin Fe^{II} ion (4.90 μ_B). The observed deviations from the spin-only values could be explained by spin–orbit coupling effects, as indicated by the EPR results on **CoRu$_2$**.

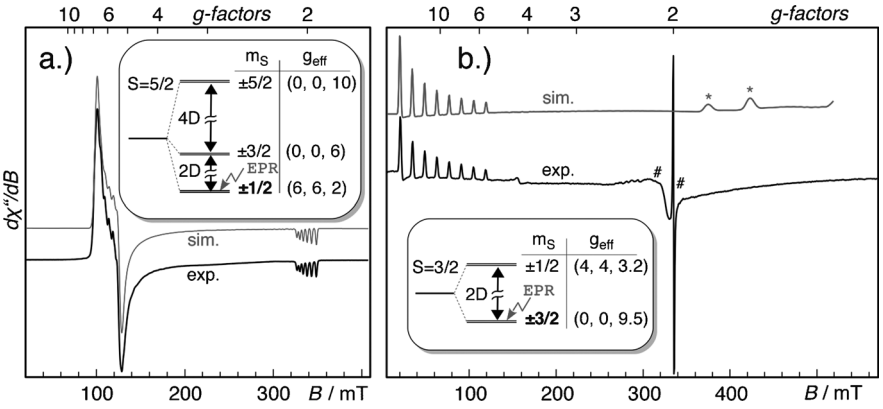

Figure 3. Experimental and simulated EPR spectra of a) [Mn{Ru(μ-H)$_3$(PTol$_3$)$_3$}$_2$] (**MnRu$_2$**) in THF at 10 K, microwave freq. = 9.47330 GHz, microwave power = 0.20 mW, modulation amplitude 8 G and b) [Co{Ru(μ-H)$_3$(PTol$_3$)$_3$}$_2$] (**CoRu$_2$**) in THF at 20 K, microwave freq. = 9.37774 GHz, microwave power = 20.0 mW, modulation amplitude 10 G. ⋆ marks artifacts from simulation cutoff effects and # marks signals from minor impurities in the EPR resonator (not in the sample; < 5% of the total experimental signal intensity). The insets show the zero-field splitting of the spin sextet and quartet multiplets for **MnRu$_2$** and **CoRu$_2$**, respectively. The effective g values, g_{eff}, for the Kramers doublets have not been used for the simulations, but are derived from the obtained spin Hamiltonian parameters given in the text; the values for the x and y direction for **CoRu$_2$** are only estimates because experimental resonances could not be detected.

The EPR spectra of **MnRu$_2$** and **CoRu$_2$** in frozen THF solution (Figure 3) are consistent with a high-spin S = 5/2 state for **MnRu$_2$** and an S = 3/2 state for **CoRu$_2$**. The spectrum of the manganese complex shows effective g values around 6 and 2, which is typical of the $|m_s = \pm 1/2>$ ground state Kramers doublet of the S = 5/2 multiplet with large axial zero-field splitting ($D \gg h\nu$, $E/D = 0$). The experimental lines show well-resolved hyperfine splitting from interactions with the ^{55}Mn nuclei (Supporting Information, Table S2). A corresponding spin Hamiltonian simulation reveals electronic g values close to the free electron value of g = 2.003, which indicates an orbital singlet ground state without first-order orbital momentum.[22] Measurements with a powder sample revealed virtually the same features for the solid material (Supporting Information, Figure S2). In contrast, the EPR spectrum of the **CoRu$_2$** shows only eight absorption-type hyperfine lines (^{59}Co, I = 7/2) from a unique effective g value at low field, $g^{eff}_{||} \approx 9.5$ (whereas the features around g = 2 are known to arise from impurities in the cavity). The other corresponding resonances of the powder spectrum at $g^{eff}{}_{\perp}$ are not observed up to fields of 600 mT. Such large g anisotropy reveals an unusual $|m_s = \pm 3/2>$ ground doublet for the S = 3/2 spin state of Co^{II} owing to strong axial negative zero-field splitting ($D < 0$, $E/D \approx 0$). This state is only weakly EPR active because of its extreme g anisotropy; nevertheless, thermal population of the excited $|m_s = \pm 1/2>$ doublet was not observed up to 40 K, which provides a constraint for D. The spectrum could be simulated with rather anisotropic electronic g values (g_z = 3.18; Supporting Information, Table S2) and large negative zero-field splitting (D = −90 cm^{-1}, E/D = 0.03). This reveals the presence of strong spin–orbit coupling for the 3d^7 ion. Similar spectra and

parameters have scarcely been observed for axial $S = 3/2$ systems.[23]

The ^{1}H NMR spectra of **FeRu** and **MRu$_2$** (M = Cr–Ni) provide little information owing to the paramagnetic nature of these species. However, the ^{1}H NMR and ^{31}P NMR data for the diamagnetic zinc complex $[Zn\{Ru(\mu\text{-}H)_3(PTol_3)_3\}_2]$ (**ZnRu$_2$**) are consistent with the solid-state structure. A characteristic high field multiplet at $\delta = -9.86$ ppm is observed for the hydride ligands in the ^{1}H NMR spectrum in [D$_8$]THF. The ^{31}P NMR spectrum shows a complex multiplet for the phosphane ligands at $\delta = -53.3$ ppm owing to P–H coupling. The ^{31}P NMR shift of **ZnRu$_2$** is close to that of the lithium salt $[Li(thf)_{2.5}\{Ru(\mu\text{-}H)_3(PTol_3)_3\}]$ (**LiRu**, $\delta = -52.7$ ppm). Complexes **MRu$_2$** (M = Cr–Ni) show weak electronic absorptions in the near UV and the visible region that we assign to d–d transitions. These absorptions show a bathochromic shift upon going from iron to nickel (**FeRu$_2$** $\lambda_{max} = 500$, **CoRu$_2$** $\lambda_{max} = 507$, **NiRu$_2$** $\lambda_{max} = 602$ nm). The absorptions of **CrRu$_2$**, **MnRu$_2$**, and **ZnRu$_2$** in the UV region are partly obscured by absorptions of the solvent (THF).

The IR spectra of **FeRu** and **MRu$_2$** in the solid state and in THF solution are similar. The spectra feature medium to strong absorptions between 1600 and 1777 cm^{-1} that can be assigned to the Ru–H vibration.[12] Ru–H absorptions in the range of 1520–1747 cm^{-1} were calculated by DFT applying the harmonic approximation for the truncated methyl-substituted models $[M\{Ru(\mu\text{-}H)_3(PMe_3)_3\}_2]$ (**MRu$_2$″**)[12] (Supporting Information, Table S9 and Figure S6). DFT calculations further predict that the M–H vibrations should be observed between 869–1055 cm^{-1}. In the experimental spectra, these bands are located in the fingerprint region and are thus difficult to identify owing to overlap with other bands. THF solutions of **LiRu**, **MnRu**, **FeRu**, and **CoRu** showed an identically low electrical conductivity as pure THF, indicating that the complexes do not dissociate in THF solutions.[12]

DFT computations (PBE-D3/def2-TZVP) on truncated models $M[Ru(\mu\text{-}H)_3(PPh_3)_3]_2$ (**MRu$_2$′**, M = Cr-Ni, Zn), where the *para*-tolyl substituents have been replaced by phenyl groups, support the structural analyses and provide a deeper insight into the bonding situation and the spin-state energetics.[12–15] The importance of intramolecular London dispersion forces in large molecular complexes has been emphasized in recent studies undertaken in our group.[24] In accord with our magnetic measurements, the high-spin configuration is favored (Table 2, entry 5). The highest energy difference ΔE between the low-spin and high-spin states was calculated for **MnRu$_2$′** ($\Delta E = +35$ kcal mol^{-1}), while ΔE is lowest for the cobalt complex **CoRu′$_2$** ($\Delta E = +6$ kcal mol^{-1}).[25] Although H^- is a strong-field ligand in terminal hydride complexes, the bridging hydride ligands in **FeRu** and **MRu$_2$′** exert a much weaker ligand field, which favors the high-spin configuration.

Spin-density plots for the trinuclear complexes **MRu$_2$′** show that the unpaired electrons of the high-spin complexes are mainly located on the central 3d atom (Supporting Information, Table S5 and Figure S4). A smaller part of the spin density is spread over the ruthenium atoms in the case of **FeRu$_2$′** and **CoRu$_2$′**. This indicates that the ruthenium atoms in these complexes display some Ru^{III} character, and the electronic structure is probably best described by two superimposed resonance configurations: Ru^{II}-M^{II}-Ru^{II} and Ru^{III}-M^0-Ru^{III}, of which the first one prevails.

Table 2: Selected Wiberg bond indices (WBI) and low-spin/high-spin energy splittings ΔE [kcal mol^{-1}] of complexes **MRu$_2$′**.

M	Cr	Mn	Fe	Co	Ni	Zn
Ru–M	> 0.03	> 0.03	0.08	> 0.03	0.12	> 0.03
Ru–H	0.60	0.35	0.47	0.55	0.55	0.80
M–H	0.04	0.33	0.16	0.06	0.09	> 0.03
Ru–P	0.95	0.85	0.88	0.92	0.89	0.92
ΔE	25	35	25	6	14	–
S[a]	2	5/2	2	3/2	1	0

[a] Sum of all electron spins.

Analysis of the Wiberg Bond Indices (WBI) gives further insight into the bonding situation in complexes **MRu$_2$′**.[26] The WBI values for the Ru–H bonds of 0.5–0.8 (Table 2) show that these bonds have significant covalent character. In contrast, the M–H bonds have WBIs of 0.03–0.33 (Table 2). These small WBIs suggest a diminished covalent character of the M–H bonds.[27] Rather small WBIs of 0.03–0.12 were also calculated for the Ru–M interactions in **MRu$_2$′**, indicating insignificant metal–metal bonding. Inspection of the localized MOs also gave no indication of metal-metal bonding (Supporting Information, Figure S5).

In conclusion, a unique series of paramagnetic polyhydride complexes $[Fe(acac)\{Ru(\mu\text{-}H)_3(PTol_3)_3\}]$ (**FeRu**) and $[M\{Ru(\mu\text{-}H)_3(PTol_3)_3\}_2]$ (**MRu$_2$**, M = Cr-Ni, Zn) has been prepared and structurally characterized. The structures of these complexes display intact *fac*-$[Ru(\mu\text{-}H)_3(PTol_3)_3]^-$ anions that coordinate to the 3d metal cation by the three hydride ligands in a symmetrical fashion. For the trinuclear complexes **MRu$_2$**, coordination of the 3d metal center (M = Cr-Ni, Zn) by two *fac*-$[Ru(\mu\text{-}H)_3(PTol_3)_3]^-$ units results in the formation of an unprecedented trigonal-antiprismatic arrangement of six hydride ligands. The complexes **FeRu** and **CrRu$_2$**–**NiRu$_2$** show large magnetic moments owing to the high-spin configuration the 3d transition-metal anion. Although open-shell transition-metal polyhydride complexes are still rare, our results indicate that such species may be more stable than previously believed.[8] Considering the rich chemistry of closed-shell polyhydrido ruthenium complexes,[7] the reaction chemistry of the new complexes **FeRu** and **MRu$_2$** is another interesting prospect that is currently being explored in our laboratories.

Received: July 3, 2012
Revised: October 1, 2012
Published online: December 3, 2012

Keywords: EPR spectroscopy · hydrides · iron · open-shell complexes · ruthenium

[1] F. Maseras, A. Lledos, E. Clot, O. Eisenstein, *Chem. Rev.* **2000**, *100*, 601–636.
[2] a) A. Dedieu, *Transition Metal Hydrides*, Wiley-VCH, Weinheim, **1992**; b) R. Poli, M. Peruzzini, *Recent Advances in Hydride Chemistry*, Elsevier, Amsterdam, **2001**, p. 557.

[3] a) F. Gloaguen, T. B. Rauchfuss, *Chem. Soc. Rev.* **2009**, *38*, 100 – 108; b) R. H. Morris, *Coord. Chem. Rev.* **2008**, *252*, 2381 – 2394; c) P. L. Holland, *Acc. Chem. Res.* **2008**, *41*, 905 – 914; d) S. Gaillard, J.-L. Renaud, *ChemSusChem* **2008**, *1*, 505 – 509; e) A. J. Hoskin, D. W. Stephan, *Coord. Chem. Rev.* **2002**, *233*, 107 – 129; f) S. Sabo-Etienne, B. Chaudret, *Coord. Chem. Rev.* **1998**, *178*, 381 – 407; g) Z. Y. Lin, M. B. Hall, *Coord. Chem. Rev.* **1994**, *135*, 845 – 879; h) G. G. Hlatky, R. H. Crabtree, *Coord. Chem. Rev.* **1985**, *65*, 1 – 48.

[4] Recent examples: a) N. L. Wieder, M. Gallagher, P. J. Carroll, D. H. Berry, *J. Am. Chem. Soc.* **2010**, *132*, 4107 – 4109; b) Y. Yu, A. R. Sadique, J. M. Smith, T. R. Dugan, R. E. Cowley, W. W. Brennessel, C. J. Flaschenriem, E. Bill, T. R. Cundari, P. L. Holland, *J. Am. Chem. Soc.* **2008**, *130*, 6624 – 6638; c) M. Baya, J. Houghton, J.-C. Daran, R. Poli, L. Male, A. Albinati, M. Gutman, *Chem. Eur. J.* **2007**, *13*, 5347 – 5359; d) V. V. Saraev, P. B. Kraikivskii, D. A. Matveev, S. N. Zelinskii, K. Lammertsma, *Inorg. Chim. Acta* **2006**, *359*, 2314 – 2320; e) F. C. Liu, J. F. Chen, S. C. Chen, K. Y. Chen, G. H. Lee, S. M. Peng, *J. Organomet. Chem.* **2005**, *690*, 291 – 300; f) E. J. Daida, J. C. Peters, *Inorg. Chem.* **2004**, *43*, 7474 – 7485.

[5] a) M. Baya, J. Houghton, J.-C. Daran, R. Poli, *Angew. Chem.* **2007**, *119*, 433 – 436; *Angew. Chem. Int. Ed.* **2007**, *46*, 429 – 432; b) B. Pleune, D. Morales, R. Meunier-Prest, P. Richard, E. Collange, J. C. Fettinger, R. Poli, *J. Am. Chem. Soc.* **1999**, *121*, 2209 – 2225; c) K. T. Smith, C. Roemming, M. Tilset, *J. Am. Chem. Soc.* **1993**, *115*, 8681 – 8689; d) O. B. Ryan, M. Tilset, V. D. Parker, *J. Am. Chem. Soc.* **1990**, *112*, 2618 – 2626.

[6] a) A. Jablonskytė, J. A. Wright, S. A. Fairhurst, J. N. T. Peck, S. K. Ibrahim, V. S. Oganesyan, C. J. Pickett, *J. Am. Chem. Soc.* **2011**, *133*, 18606 – 18609; b) J. Harmer, C. Finazzo, R. Piskorski, S. Ebner, E. C. Duin, M. Goenrich, R. K. Thauer, M. Reiher, A. Schweiger, D. Hinderberger, B. Jaun, *J. Am. Chem. Soc.* **2008**, *130*, 10907 – 10920; c) P. E. M. Siegbahn, J. W. Tye, M. B. Hall, *Chem. Rev.* **2007**, *107*, 4414 – 4435; d) R. Y. Igarashi, M. Laryukhin, P. C. Dos Santos, H.-I. Lee, D. R. Dean, L. C. Seefeldt, B. M. Hoffman, *J. Am. Chem. Soc.* **2005**, *127*, 6231 – 6241; e) R. Mejia-Rodriguez, D. Chong, J. H. Reibenspies, M. P. Soriaga, M. Y. Darensbourg, *J. Am. Chem. Soc.* **2004**, *126*, 12004 – 12014; f) S. Foerster, M. Stein, M. Brecht, H. Ogata, Y. Higuchi, W. Lubitz, *J. Am. Chem. Soc.* **2003**, *125*, 83 – 93.

[7] a) H. Suzuki, *Eur. J. Inorg. Chem.* **2002**, 1009 – 1023; b) G. Lavigne, *Angew. Chem.* **2012**, *124*, 5894 – 5896; *Angew. Chem. Int. Ed.* **2012**, *51*, 5794 – 5796.

[8] a) R. M. Hiney, A. B. Chaplin, J. Harmer, J. C. Green, A. S. Weller, *Dalton Trans.* **2010**, *39*, 1726 – 1733; b) S. K. Brayshaw, A. Harrison, J. S. McIndoe, F. Marken, P. R. Raithby, J. E. Warren, A. S. Weller, *J. Am. Chem. Soc.* **2007**, *129*, 1793 – 1804; c) J. D. Jewson, L. M. Liable-Sands, G. P. A. Yap, A. L. Rheingold, K. H. Theopold, *Organometallics* **1999**, *18*, 300 – 305; d) M. E. Smith, R. A. Andersen, *Organometallics* **1996**, *15*, 2680 – 2682; e) R. A. Heintz, T. F. Koetzle, R. L. Ostrander, A. L. Rheingold, K. H. Theopold, P. Wu, *Nature* **1995**, *378*, 359 – 362; f) R. A. Heintz, R. L. Ostrander, A. L. Rheingold, K. H. Theopold, *J. Am. Chem. Soc.* **1994**, *116*, 11387 – 11396; g) J. L. Kersten, A. L. Rheingold, K. H. Theopold, C. P. Casey, R. A. Widenhoefer, C. Hop, *Angew. Chem.* **1992**, *104*, 1364 – 1366; *Angew. Chem. Int. Ed. Engl.* **1992**, *31*, 1341 – 1343; h) R. A. Heintz, B. S. Haggerty, H. Wan, A. L. Rheingold, K. H. Theopold, *Angew. Chem.* **1992**, *104*, 1100 – 1102; *Angew. Chem. Int. Ed. Engl.* **1992**, *31*, 1077 – 1079.

[9] a) A. S. C. Chan, H.-S. Shieh, *J. Chem. Soc. Chem. Commun.* **1985**, 1379 – 1380; b) R. Wilczynski, W. A. Fordyce, J. Halpern, *J. Am. Chem. Soc.* **1983**, *105*, 2066 – 2068.

[10] a) D. Alvarez, E. G. Lundquist, J. W. Ziller, W. J. Evans, K. G. Caulton, *J. Am. Chem. Soc.* **1989**, *111*, 8392 – 8398; b) J. T. Poulton, K. Folting, K. G. Caulton, *Organometallics* **1992**, *11*, 1364 – 1372.

[11] CCDC CCDC 888716 (**LiRu**), 888717 (**FeRu**), 888718 (**$CrRu_2$**), 888719 (**$MnRu_2$**), 888720 (**$FeRu_2$**), 888721 (**$CoRu_2$**), 888722 (**$NiRu_2$**), and 888723 (**$ZnRu_2$**) contain the supplementary crystallographic data for this paper. These data can be obtained free of charge from The Cambridge Crystallographic Data Centre via www.ccdc.cam.ac.uk/data_request/cif.

[12] See Supporting Information for details.

[13] a) *Turbomole version 5.9*, R. Ahlrichs, **2008**; b) F. Weigend, R. Ahlrichs, *Phys. Chem. Chem. Phys.* **2005**, *7*, 3297 – 3305.

[14] a) S. Grimme, *J. Comput. Chem.* **2006**, *27*, 1787; b) S. Grimme, J. Antony, S. Ehrlich, H. Krieg, *J. Chem. Phys.* **2010**, *132*, 154104; c) J. P. Perdew, K. Burke, M. Ernzerhof, *Phys. Rev. Lett.* **1996**, *77*, 3865.

[15] The optimized structure of $[Zn\{Ru(\mu\text{-}H)_3(PTol_3)_3\}_2]$ (**$ZnRu_2$**) is very similar to the optimized structure of $[Zn\{Ru(\mu\text{-}H)_3(PPh_3)_3\}_2]$ (**$ZnRu_2'$**), showing that the *para*-methyl substituents on the phosphane ligands have little structural effect.

[16] L. Brammer, W. T. Klooster, F. R. Lemke, *Organometallics* **1996**, *15*, 1721 – 1727.

[17] For related homoleptic second- and third-row transition-metal hydride complexes, see: a) S. K. Brayshaw, J. C. Green, R. Edge, E. J. L. McInnes, P. R. Raithby, J. E. Warren, A. S. Weller, *Angew. Chem.* **2007**, *119*, 7990 – 7994; *Angew. Chem. Int. Ed.* **2007**, *46*, 7844 – 7848; b) X. Li, J. Baldamus, M. Nishiura, O. Tardif, Z. Hou, *Angew. Chem.* **2006**, *118*, 8364 – 8368; *Angew. Chem. Int. Ed.* **2006**, *45*, 8184 – 8188; c) J. P.-K. Lau, W.-T. Wong, *Dalton Trans.* **2005**, 2579 – 2587; d) F. Bachechi, *J. Organomet. Chem.* **1994**, *474*, 191 – 197; e) F. Bachechi, C. Bianchini, A. Meli, *Inorg. Chim. Acta* **1993**, *213*, 269; f) A. P. Ginsberg, S. C. Abrahams, P. Marsh, K. Ataka, C. R. Sprinkle, *J. Chem. Soc. Chem. Commun.* **1984**, 1321 – 1323; g) K. Knox, A. P. Ginsberg, *Inorg. Chem.* **1964**, *3*, 555 – 558; h) S. C. Abrahams, A. P. Ginsberg, K. Knox, *Inorg. Chem.* **1964**, *3*, 558 – 567.

[18] a) R. Bau, M. Y. Chiang, D. M. Ho, S. G. Gibbins, T. J. Emge, T. F. Koetzle, *Inorg. Chem.* **1984**, *23*, 2823 – 2829; b) J. Huot, S. Boilya, E. Akibab, R. Schulz, *J. Alloys Compd.* **1998**, *280*, 306 – 309; c) B. Huang, F. Bonhomme, P. Selvam, K. Yvon, P. Fischer, *J. Less-Common. Met.* **1991**, *171*, 301.

[19] M. Maekawa, M. Römelt, C. G. Daniliuc, P. G. Jones, P. S. White, F. Neese, M. D. Walter, *Chem. Sci.* **2012**, *3*, 2972 – 2979.

[20] S. Pfirrmann, C. Limberg, C. Herwig, C. Knispel, B. Braun, E. Bill, R. Stösser, *J. Am. Chem. Soc.* **2010**, *132*, 13684 – 13691.

[21] M. C. Lipke, T. D. Tilley, *Angew. Chem.* **2012**, *124*, 11277 – 11283; *Angew. Chem. Int. Ed.* **2012**, *51*, 11115 – 11121.

[22] The axial zero-field splitting parameter D could not be determined because for vanishing rhombicity, $E/D \approx 0$, only the $|m_s = \pm 1/2>$ Kramers doublet is EPR-active.

[23] R. E. Cowley, N. A. Eckert, S. Vaddadi, T. M. Figg, T. R. Cundari, P. L. Holland, *J. Am. Chem. Soc.* **2011**, *133*, 9796 – 9811.

[24] a) S. Grimme, J.-P. Djukic, *Inorg. Chem.* **2011**, *50*, 2619 – 2628; b) S. Grimme, J.-P. Djukic, *Inorg. Chem.* **2010**, *49*, 2911 – 2919.

[25] The low-spin states showed some spin contamination (see the Supporting Information, Table S8), which artificially lowers the energy of the low-spin complexes and reduce the energy difference ΔE. DFT-GGA functionals underestimate the energy splitting systematically; therefore, the error owing to the spin contamination further decreases somewhat the energy splitting ΔE. See the Supporting Information for details.

[26] K. B. Wiberg, *Tetrahedron* **1968**, *24*, 1083-1096.

[27] For the manganese complex **$MnRu_2'$**, we found a rather large WBI of 0.33 for the Mn–H interactions compared to the other metals. The magnitude of the WBI persist even greater with other density functionals (see Table 2 and the Supporting Information).

